NANOTECHNOLOGY ENABLED HYDROGEN GAS SENSING

Atkin, P.[a], Hashtroudi, H.[a], Mackinnon, I.D.R.[b] and Shafiei, M.[a,b]

[a]Faculty of Science, Engineering and Technology, Swinburne University of Technology, Hawthorn, VIC 3122, Australia, mshafiei@swin.edu.au

[b]Institute for Future Environments, Queensland University of Technology (QUT), Brisbane, QLD 4001, Australia, ian.mackinnon@qut.edu.au

ABSTRACT

An important contribution to industry standards and to effective installation of hybrid renewable energy systems is evaluation of hydrogen (H_2) monitoring techniques under pilot-scale and/or real-world conditions. We have designed a hybrid system to integrate solar power, electrolysis and hydrogen fuel cell components in a DC micro-grid with capacity to evaluate novel nanomaterials for enhanced H_2 gas sensing performance. In general, enhanced hydrogen sensing performance is evaluated by high sensitivity, selectivity and stability as well as low power consumption. Unique properties, such as high surface area to volume ratio, a large number of surface active sites, high specific surface area and reactivity are key attributes of nanomaterials used for gas sensing. These attributes enable sensors to be embedded in Internet-of-Things applications or in mobile systems. With rapid development of hydrogen-based technologies for clean energy applications, there remains a requirement for faster, accurate and selective H_2 sensors with low cost and low power consumption. Operating principles for these sensors include catalytic, thermal conductivity, electrochemical, resistance based, optical and acoustic methods. In this paper, we review performance of H_2 gas sensors based on conductometric devices operating at room temperature up to 200 °C. The focus of this work includes nanostructured metal oxides, graphene materials and transition metal dichalcogenides employed as sensing materials.

Keywords: Hydrogen gas sensors; nanomaterials; sensing techniques; low temperature

1.0 INTRODUCTION

In recent years, recognition of resource constraints and efforts to reduce global emissions have encouraged development of low- or zero- carbon solutions to energy production and storage. In Australia, conventional fossil fuel methods now compete with alternative energy sources due to increasing costs and environmental issues that arise from network constraints and lack of capacity. Hydrogen is an alternative energy source that can be produced from a range of existing and emerging technologies, such as steam reforming or electrolysis that are viable at regional scales. In addition, hydrogen is suitable for diverse end-use applications supporting decarbonisation in the transport, chemicals, construction and power industries. More importantly, as shown schematically in Figure 1, hydrogen enables linkages between energy generation and use to deliver system flexibility for constrained networks.

Hydrogen produced by renewable energy sources, often termed "green hydrogen", has a high energy storage capacity, a high relative energy density (~3× diesel fuel) and minimal harmful or polluting products [1] when used to generate electricity (*e.g.* via fuel cells). However, the hazards associated with H_2 gas are also well documented [2]. Combustible at concentrations in air between 4% and 75%, and with a very low minimum ignition energy (at optimal combustion concentration in air) of less than 0.02 mJ, H_2 is a gas that requires strict and thorough safety methods in place if it is to be put to widespread use [3-5]. The tremendous research effort devoted to development of hydrogen gas sensors is reflected in the growing number of relevant publications as shown in Fig. 2.
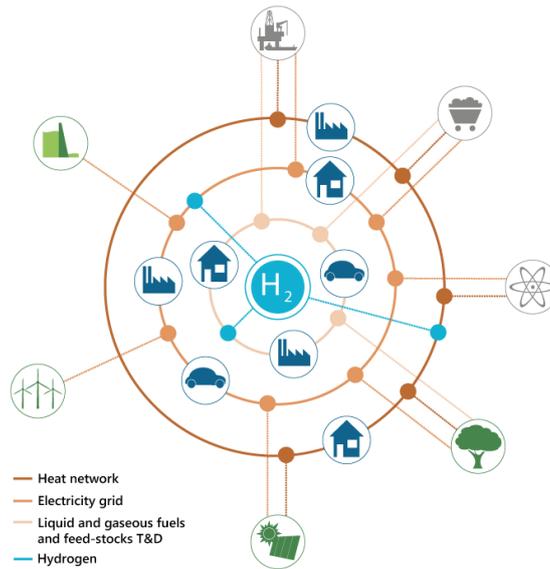
Figure 1. Schematic showing the important role for hydrogen in future low-carbon, energy generation and distribution networks. (Source: https://www.iea.org/tcep/energyintegration/hydrogen/)
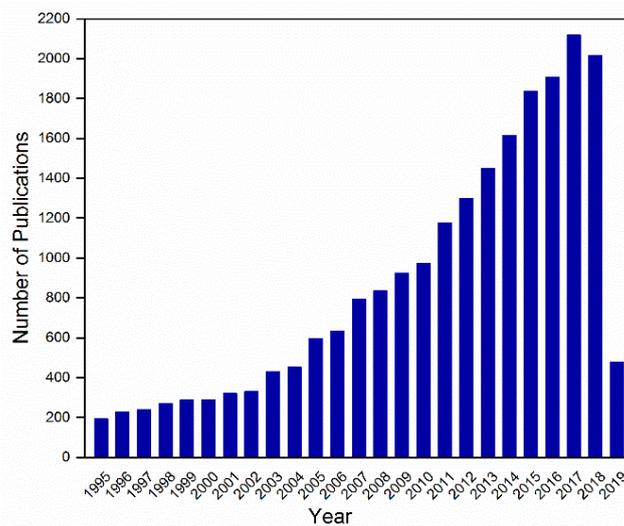

Figure 2. Number of journal article publications on the topic of hydrogen sensors (Source: Web of Science searched on 25th March 2019).

The detection of H_2 gas in the atmosphere is of great importance in maintaining safety at all stages of H_2 production, storage and use. However, several issues set H_2 apart from other commercially available gases. Sulphur-containing odorants typically added to commercially available gases (such as ethyl mercaptan) are unsuitable for use with H_2, as these gases are much heavier and quickly separate from the H_2 upon release [6]. Furthermore, these odorants are known to contaminate fuel cells, which are an important application of H_2 currently under consideration [7, 8]. A new class of H_2 sensors is now emerging, in which the unique properties found in nanomaterials such as high surface area to volume ratio, number of active sites and reactivity can be harnessed. These properties can help to develop sensors with improved performance via lower working temperature (i.e. lower power consumption), higher sensitivity, lower limit of detection (LoD), and improved selectivity, to name a few properties. With these advances in mind, it now becomes feasible to apply recently-developed H_2 sensors in situations where the target gas is detected at low temperatures, even as low as room temperature (RT). Detection of H_2 gas at such temperatures was previously very difficult, in part due to the difficulty for electrons to be excited and to interact with the sensing material [9].

In this review, nanomaterials showing promise for the application of H_2 sensing at low temperatures ranging from RT up to 200°C are presented in an exploration of the field as it currently stands. This evaluation is a critical step in the selection of new materials for benchmark trials in our proposed hybrid renewable energy hydrogen production pilot plant. Materials from the three most commonly reported categories of metal oxides (MOxs), transition metal dichalcogenides (TMDs) and graphene/reduced graphene oxide (rGO) are discussed. Conductometric sensors are the main focus, due to the inherent favourable characteristics of low cost, ease of miniaturisation, and simplicity of fabrication and use [10]. In simplest terms, resistive sensing operates by detecting a change in the resistivity (or conductivity) of the sensing material component in a transducer. This change can be brought about in a range of different ways, but typically occurs when target gas molecules interact covalently or non-covalently with the sensing material surface [11].

Materials with an electronic bandgap are intrinsically useful in conductometric sensing applications. However, problems arise when relatively narrow bandgap materials (such as WO_3 or MoS_2) are exposed to higher temperatures. Under such conditions, excitation of valence electrons due to heating can reduce the resistance of a semiconducting material to the point that reduction of resistance due to gas molecule adsorbance can no longer be detected. Furthermore, lower operating temperatures are preferable when designing processes from an economic standpoint. With these concerns in mind, it is necessary to explore materials that can be employed in gas sensing at low temperatures. In many cases, semiconducting materials have shown improved sensitivity when employed in a hybrid material along with noble metal structures (preferred over other metals to avoid oxidation), where H_2 molecules are easily dissociated, forming a dipole layer on the metal surface. Typically, Pt and Pd have been the most commonly used metals, showing significant improvements in the H_2 sensing response of their complementary sensing materials [9, 12, 13].

2.0 H_2 SENSING NANOMATERIALS

2.1 MOx Based H_2 Gas Sensors

Gas sensing mechanisms for metal oxide semiconductor-based conductometric devices involve a number of steps. Typically, O_2 molecules in air are adsorbed onto the semiconductor surface, dissociating and forming oxygen ions while electrons within the semiconducting material are transferred to the oxygen molecules. With this reduction in free electron concentration, the resistance of the semiconductor increases.[14] Upon exposure to H_2 gas, electrons from H_2 molecules transfer from the gas to the semiconducting oxide surface, producing H^+ ions, due to the work function of semiconducting materials being higher than the affinity of the H_2 molecules. H^+ ions are then able to react with the chemisorbed oxygen ions to form H_2O, releasing the electrons previously held by oxygen ions back into the semiconductor. In terms of sensing output, the result of this electron transfer depends on the type of semiconductor. While p-type semiconductors will experience a reduction in hole concentration and a subsequent increase in resistance, n-type materials will conversely undergo an increase in electron concentration and the resistance will decrease accordingly [14-18].

Different types of semiconducting MOx with nanostructured morphology including SnO_2, WO_3, MoO_3, ZnO and TiO_2 have shown promising results for H_2 sensing [2, 19-27]. Among these materials, MOx nanowires have proven applications in H_2 sensing at RT when surface functional structures are added, as demonstrated by Ren *et al.* [20] in 2016. In this work, TiO_2 nanowires showed no detectable response to H_2. However, functionalisation with PdAu nanoparticles (NPs) resulted in a hybrid material with high sensitivity of 350, a low LoD of 5 ppm, and a rapid response time (21 s) at RT [20]. Thin films of WO_3 were found by Zhang *et al.* [22] to be unreactive with H_2 gas at low temperatures, but with the addition of Pt NPs were able to respond to H_2 concentrations as low as 50 ppm at 150°C (albeit with slow response and recovery times of 452 and 660 s, respectively). Similarly, SnO_2 thin films exhibit prohibitively poor sensitivity to low concentrations of H_2 gas, but functionalisation can greatly improve performance. Nguyen *et al.* [19] showed that thin films of SnO_2 functionalised with microscale Pd

islands had a quick response at only 100 ppm H_2 at 150°C. Although Pd itself has been shown many times to be an excellent RT H_2 gas sensing material, the sensitivity can be poor in some cases. In addition, the metal itself is expensive, and prone to degradation over repeated H_2 adsorption-desorption cycles [5, 10, 28]. An overall comparison of the materials discussed here is shown in Table 1.

Table 1. H_2 sensing properties of some MOx nanomaterials.

Material	Morphology	Synthesis Method	Hybrid Material	T(°C)	H_2 Conc. (ppm)	Response time (s)	Recovery time (s)	Response Calculation	Response	LoD (ppm)
SnO$_2$ [19]	Thin films	Reactive sputtering	Pd islands	150	100	50	-	V_g/V_0	1.9	50
WO$_3$ [22]	Thin films	Electroless deposition	Pt NPs	150	50	452	660	$(R_0 - R_g)/R_0$	2.09	50
TiO$_2$ [20]	Nanowires	Hydrothermal	PdAu NPs	RT	5	21	-	$(I_g - I_0)/I_0$	350	5
ZnO [21]	Nanosheets	Thermal oxidation	-	175	10	11.5	14.5	R_0/R_g	1.089	0.5
SnO$_2$-MoS$_2$ [2]	Nanosheets	Hydrothermal	Pd-SnO$_2$/MoS$_2$	RT	100	15	12	$(R_0 - R_g)/R_0$	1.8	30

Response calculation methods are given as reported for each material, where V = potential, R = resistance, and I = current, and 0 and g represent the conditions before and after the introduction of H_2 to the system, respectively. T = operating temperature.

2.2 TMD Based H_2 Gas Sensors

As with MOxs, the mechanism of gas sensing in TMD conductometric devices is based on charge transfer. However, in the case of TMDs, the target gas molecules are adsorbed directly on to the sensing material, donating electrons to the conduction band of the TMD and increasing the conductivity [15, 29]. The active sites for charge transfer in TMDs are typically either defects in the material, or the p-orbitals of chalcogenide atoms [11]. Unfortunately, the promising sensing capabilities of TMDs are offset by the slow gas desorption process at RT, which often results in long recovery times [15]. Liu *et al.* [4] demonstrated application of pristine MoS$_2$ deposited on Si substrates for H_2 sensing, showing a relatively high response (15.4) and fast response and recovery to 5,000 ppm H_2 balanced in air at RT due to the *p-n* junction formed between the two materials. Kuru and his group's work [5, 30] with MoS$_2$ (in 2015) and Pd NP-decorated WS$_2$ nanosheets (in 2016) showed typical response and recovery times for TMD based H_2 sensors, with response time decreasing and recovery time increasing with increasing H_2 concentration. Additionally, the 2015 work on MoS$_2$ based H_2 sensors showed that recovery times could be reduced by annealing the sensing materials, at the expense of sensor response [30]. Two-dimensional (2D) TMDs have been reportedly prepared using several different routes, with exfoliation methods typically preferable to growth on a substrate due to the higher surface area to volume ratio. Morphology plays a crucial role here, with thickness, lateral dimensions and orientation all affecting surface area. This is reflected in the comparison made between TMD gas sensing materials shown in Table 2.

Table 2. H_2 sensing properties of some TMD nanomaterials.

Material	Morphology	Synthesis Method	Hybrid Material	T (°C)	H_2 Conc. (ppm)	Response time (s)	Recovery time (s)	Response Calculation	Response	LoD (ppm)
MoS_2 [31]	NPs	Hydrothermal	Pt-doped TiO_2-MoS_2	100	2000	150	310	-	74.90%	50
MoS_2 [32]	Nanosheets	Mechanical exfoliation	Various metal NPs	RT	3	>900	-	$(I_g - I_0)/I_0$	5	3
MoS_2 [30]	Nanosheets	Mechanical exfoliation	Pd NPs	RT	50000	40	83	R_0/R_g	10	500
WS_2 [5]	Nanosheets	Mechanical exfoliation	Pd NPs	RT	50000	119	370	R_0/R_g	7.8	500
MoS_2-Si [4]	Thin films	Magnetron sputtering	-	RT	5000	105	444	$I_0/I_g - 1$	15.4	5000
MoS_2-SiO_2 [33]	Thin films	Magnetron sputtering	Pd NPs	RT	5000	36.8	35.3	I_g/I_0	570	5000

Response calculation methods are given as reported for each material, where R = resistance and I = current, and 0 and g represent the conditions before and after the introduction of H_2 to the system, respectively. T = operating temperature.

2.3 Graphene and rGO Based H_2 Gas Sensors

A range of gas sensing mechanisms for graphene have been reported, typically involving π-π interaction, charge transfer or van der Waals forces with the sp^2 orbitals of carbon atoms or with defects in the material [11]. Although the interaction of H_2 with pristine graphene is poor due to the weak adsorption energy of the gas, this interaction can be improved by the introduction of defects, dopants or by functionalisation [11, 29]. Many carbon nanostructures have therefore shown promise in gas sensing applications. Carbon nanotubes (CNTs) were found to have excellent sensing capabilities toward several gases including H_2, but with the drawback that bundled CNTs had slow recovery times, and the production of an individual CNT is very difficult at this stage [13, 34]. CNTs decorated with Pd NPs are found to have much faster sensing response and recovery times at RT, compared with both undecorated CNTs and Pd NPs [35, 36].

rGO thin films have been reported in H_2 sensing applications with and without the addition of functional structures [37-39]. In general, rGO is prepared using Hummers' Method (or modifications thereof) followed by hydrothermal treatment. As in the case of MOxs and TMDs discussed earlier, the formation of a hybrid material including rGO and Pd has been shown to drastically improve sensing response, while a modest improvement can also be achieved via the introduction of ZnO nanorods [37, 38, 40]. H_2 sensing materials based on rGO showed faster response and recovery times, lower LoD and stronger response compared with those based on graphene, as demonstrated in Table 3.

The exception to this trend is the material reported by Zhang *et al.* [41] in 2015, where the H_2 sensing properties of graphene were enhanced, via the addition of SnO_2 NPs, to the degree that it outperforms every other material explored in this category. In the case of graphene nanosheets functionalised with noble metal NPs, it can be observed from the work of Kaniyoor *et al.* [42] and Chung *et al.* [43] that CVD-grown graphene appears to be superior in terms of response time and LoD over graphene prepared by thermal exfoliation. This observation is made under the assumption that the Pt NPs used in the former work yield similar enhancement to that of the Pd NPs used in the latter work, and that NPs are applied in similar quantities. The most likely explanations for this difference in performance are the greater surface area to volume ratio of the CVD-prepared graphene (prepared by Chung *et al.*), and the presence of many defects in the thermally oxidation-prepared material (Kaniyoor *et al.*).

Table 3. H_2 sensing properties of some graphene-based nanomaterials.

Material	Morphology	Synthesis Method	Hybrid Material	T (°C)	H_2 Conc. (ppm)	Response time (s)	Recovery time (s)	Response Calc.	Response	LoD (ppm)
rGO [38]	Thin films	Hummers', Hydrothermal	-	RT	160	20	10	$(R_0 - R_g)/R_0$	0.045	30
rGO [37]	Thin films	Hummers', Hydrothermal	Pd-WO$_3$ nanoribbons	RT	100	52	155	$(G - G_0)/G_0$	38	20
rGO [40]	Thin films	Hummers', Hydrothermal	ZnO nanorods	150	200	22	90	R_0/R_g	3.5	10
Graphene [41]	Nanosheets	Mechanical exfoliation	SnO$_2$ NPs	50	100	1.1	1.1	I_g/I_0	2.4	1
Graphene [42]	Nanosheets	Thermal exfoliation	Pt NPs	RT	40000	540	-	$(R_g - R_0)/R_g$	16%	-
Graphene [44]	Nanosheets	Chemical polymerization	Polyaniline	RT	10000	60*	300*	$(R_g - R_0)/R_0$	16.57	600
Graphene [45]	Nanosheets	Chemical GO reduction	Pt-Graphene-SiC	100	10000	120*	300*	$V_g - V_0$	63 mV	600
Graphene [46]	Nanoribbons	Mechanical exfoliation	Pd NPs	RT	8000	6	44	$(R_g - R_0)/R_0$	77%	40
Graphene [43]	Nanosheets	CVD	Pd NPs	RT	1000	60*	>1800	$(R_g - R_0)/R_0$	33%	20

Response calculation methods are given as reported for each material, where G = conductance, V = potential, R = resistance, and I = current, and 0 and g represent the conditions before and after the introduction of H_2 to the system, respectively. T = operating temperature.

3.0 DISCUSSION

At first glance, it would appear that MOxs possess the most desirable characteristics in applications for H_2 sensing at low temperatures. However, this class of nanomaterials gives best results in this application either when coupled with noble metal nanoparticles (most commonly Pd) or when a mild degree of heating is applied [19, 21]. The use of heating in the former case, or expensive noble metals in the latter, may not be considered when cost is a factor. These restrictions also apply to several of the highest-performing TMDs and graphitic materials, which also rely on the addition of noble metal nanostructures or heating [15, 28, 30, 32]. We have identified one case, in the work by Liu *et al.* [4], where MoS$_2$ has been used for high-performance H_2 sensing without the addition of other functional nanostructures; however in this case the sensing performance was enhanced via a heterojunction effect with the Si substrate.

It is difficult to draw a direct comparison between varying morphologies of a given sensing material, due mainly to the large number of variable factors in reported materials. However, from an overall perspective of the materials explored here, some observations can be made that may assist in selection of morphology for a given application. While many H_2 sensing thin films or nanosheets show a requirement for heating above 100°C in order to achieve desirable performance, the one-dimensional (1D) nanowires and nanoribbons reported by Ren and Liu [20] and Johnson *et al.* [46] are able to detect very low H_2 concentrations, with very fast response and recovery times, at RT. In the former case, the TiO$_2$ nanowires are able to outperform thin films of SnO$_2$ or WO$_3$ in speed and operating temperature, considering that all these materials are functionalised with noble metal nanostructures [19, 22]. This advantage could be attributed to the higher surface area to volume ratio and chemisorptive properties of the 1D structures [9, 13, 47].

Regarding thin films, it is difficult to discern any trend related to morphology. There has been some discussion around the effect of film thickness on gas sensing performance, where peak sensing performance is reached at some optimal thickness. While Cha *et al.* [48] suggest that crystallinity may deteriorate at thicknesses below 30 nm, Yamazaki *et al.* [49] argue that their amorphous SnO$_2$ sensor

showed greater performance, despite not being crystalline at all [48, 49]. The exact mechanism here remains unclear, but is likely to depend on the individual materials and conditions. However, it is known that sensitivity typically increases as thickness of the gas sensing material decreases and approaches that of the electron depletion layer [50].

In all three of the categories of H_2 sensing nanomaterials discussed here, we find that the most favourable sensing performances reported to date rely on functionalisation with some other nanostructure, as shown in Table 4. Of the materials compared in this review, the work of Zhang *et al.*[41], in which SnO_2 NPs are used to functionalise graphene nanosheets, reports the only material to show all of the attributes necessary for a low-cost, low-temperature, high-performing H_2 sensor.

Table 4. Comparison of H_2 sensing capabilities of highest-performing materials from each material category outlined previously.

Material	Morphology	Hybrid Material	T (°C)	H_2 Conc. (ppm)	Response time (s)	Recovery time (s)	LoD (ppm)
TiO_2 [20]	Nanowires	PdAu NPs	RT	5	21	-	5
ZnO [21]	Nanosheets	-	175	10	11.5	14.5	0.5
SnO_2-MoS_2 [2]	Nanosheets	Pd-SnO_2/MoS_2	RT	100	15	12	30
MoS_2 [30]	Nanosheets	Pd NPs	RT	50000	40	83	500
MoS_2-Si [4]	Thin films	-	RT	5000	105	444	5000
Graphene [41]	Nanosheets	SnO_2 NPs	50	100	1.1	1.1	1
rGO [37]	Thin films	Pd-WO_3 nanoribbons	RT	100	52	155	20
rGO [40]	Thin films	ZnO	150	200	22	90	10

T = operating temperature.

4.0 CONCLUSION

The gas sensing performance of 2D MOxs has been shown to be generally superior to that of 2D TMDs and graphene, when the pristine material is considered. However, with the addition of functional nanostructures, the performance of the base 2D gas sensor materials can be dramatically enhanced. The morphology of the base sensing material does appear to play a role in its sensing properties, mainly in the effect it has on surface area to volume ratio. Future work may be necessary to clarify the extent of this enhancement, as the additional effort required to prepare materials with higher surface area for gas adsorption/desorption may outweigh the benefits.

While several methods have been shown that enhance the sensing performance of MOxs, TMDs and graphene materials, the most effective involve introducing nanostructures of noble metals or metal oxides. The great benefits of the former have been proven many times over. However, the cost of noble metals such as Pd and Pt may be prohibitively expensive for large-scale production. In the interests of minimal financial and energy costs, the challenge is to explore enhancement methods that do not require excessive energy input or the addition of expensive functional materials. Methods involving the addition of MOx NPs to graphene, such as the encouraging work reported by Zhang *et al.* [41], currently show the greatest promise in this direction. With further work on this aspect of H_2 sensing nanomaterials, it is likely that performance can continue to improve.

References

1. Colella, W.G., Jacobson, M.Z., and Golden, D.M., Switching to a U.S. hydrogen fuel cell vehicle fleet: The resultant change in emissions, energy use, and greenhouse gases. *J. Power Sources*. **150**, 2005, pp. 150-181.
2. Zhang, D., et al., Room temperature hydrogen gas sensor based on palladium decorated tin oxide/molybdenum disulfide ternary hybrid via hydrothermal route. *Sens. Actuators B Chem.* **242**, 2017, pp. 15-24.
3. Ono, R. and Oda, T., Spark ignition of hydrogen-air mixture. *J. Phys. Conf. Ser.* **142**, 2008, pp. 012003.
4. Liu, Y., et al., Hydrogen gas sensing properties of MoS_2/Si heterojunction. *Sens. Actuators B Chem.* **211**, 2015, pp. 537-543.
5. Kuru, C., et al., High-performance flexible hydrogen sensor made of WS_2 nanosheet–Pd nanoparticle composite film. *Nanotechnology*. **27**(19), 2016, pp. 195501.
6. Kopasz, J.P., Fuel cells and odorants for hydrogen. *Int. J. Hydrog. Energy*. **32**(13), 2007, pp. 2527-2531.
7. de Wild, P.J., et al., Removal of sulphur-containing odorants from fuel gases for fuel cell-based combined heat and power applications. *J. Power Sources*. **159**(2), 2006, pp. 995-1004.
8. Imamura, D., Akai, M., and Watanabe, S., Exploration of hydrogen odorants for fuel cell vehicles. *J. Power Sources*. **152**, 2005, pp. 226-232.
9. Luo, Y., et al., Hydrogen sensors based on noble metal doped metal-oxide semiconductor: A review. *Int. J. Hydrog. Energy*. **42**(31), 2017, pp. 20386-20397.
10. Zhang, J., et al., Nanostructured Materials for Room-Temperature Gas Sensors. *Adv. Mater.* **28**(5), 2016, pp. 795-831.
11. Meng, Z., et al., Electrically-Transduced Chemical Sensors Based on Two-Dimensional Nanomaterials. *Chem. Rev.* **119**(1), 2019, pp. 478-598.
12. Armgarth, M., Söderberg, D., and Lundström, I., Palladium and platinum gate metal-oxide-semiconductor capacitors in hydrogen and oxygen mixtures. *Appl. Phys. Lett.* **41**(7), 1982, pp. 654-655.
13. Bindra, P. and Hazra, A., Capacitive gas and vapor sensors using nanomaterials. *J. Mater. Sci. Mater. Electron.* **29**(8), 2018, pp. 6129-6148.
14. Boudiba, A., et al., Sensing mechanism of hydrogen sensors based on palladium-loaded tungsten oxide (Pd–WO_3). *Sens. Actuators B Chem.* **187**, 2013, pp. 84-93.
15. Joshi, N., et al., A review on chemiresistive room temperature gas sensors based on metal oxide nanostructures, graphene and 2D transition metal dichalcogenides. *Microchim. Acta*. **185**(4), 2018, pp. 213.

16. Perfecto, T.M., Zito, C.A., and Volanti, D.P., Design of nanostructured $WO_3 \cdot 0.33H_2O$ via combination of ultrasonic spray nozzle and microwave-assisted hydrothermal methods for enhancing isopropanol gas sensing at room temperature. *CrystEngComm*. **19**(20), 2017, pp. 2733-2738.

17. Ab Kadir, R., et al., Electrospun Granular Hollow SnO_2 Nanofibers Hydrogen Gas Sensors Operating at Low Temperatures. *J. Phys. Chem. C*. **118**(6), 2014, pp. 3129-3139.

18. Shimizu, Y. and Egashira, M., Basic Aspects and Challenges of Semiconductor Gas Sensors. *MRS Bull.* **24**(6), 1999, pp. 18-24.

19. Nguyen, V.D., et al., Effects of gamma irradiation on hydrogen gas-sensing characteristics of $Pd–SnO_2$ thin film sensors. *Int. J. Hydrog. Energy*. **40**(36), 2015, pp. 12572-12580.

20. Ren, S. and Liu, W., One-step photochemical deposition of PdAu alloyed nanoparticles on TiO_2 nanowires for ultra-sensitive H_2 detection. *J. Mat. Chem. A*. **4**(6), 2016, pp. 2236-2245.

21. Tonezzer, M. and Iannotta, S., H_2 sensing properties of two-dimensional zinc oxide nanostructures. *Talanta*. **122**, 2014, pp. 201-208.

22. Zhang, C., et al., H_2 sensors based on WO_3 thin films activated by platinum nanoparticles synthesized by electroless process. *Int. J. Hydrog. Energy*. **38**(6), 2013, pp. 2929-2935.

23. Shafiei, M., et al., Improving the hydrogen gas sensing performance of Pt/MoO_3 nanoplatelets using a nano thick layer of La_2O_3. *Sens. Actuators B Chem.* **187**, 2013, pp. 267-273.

24. Shafiei, M., et al., A Hydrogen Gas Sensor Based on $Pt/Nanostructured WO_3/SiC$ Schottky Diode. *Sensor Lett.* **9**(1), 2011, pp. 11-15.

25. Shafiei, M., et al., Reversed bias Pt/nanostructured ZnO Schottky diode with enhanced electric field for hydrogen sensing. *Sens. Actuators B Chem.* **146**(2), 2010, pp. 507-512.

26. Yu, J., et al., Enhancement of electric field properties of $Pt/nanoplatelet MoO_3/SiC$ Schottky diode. *J. Phys. D: Appl. Phys.* **43**(2), 2009, pp. 025103.

27. Yu, J., et al., Hydrothermally formed functional niobium oxide doped tungsten nanorods. *Nanotechnology*. **24**(49), 2013, pp. 495501.

28. Hughes, R.C., et al., Thin-film palladium and silver alloys and layers for metal-insulator-semiconductor sensors. *J. Appl. Phys.* **62**(3), 1987, pp. 1074-1083.

29. Varghese, S.S., et al., Two-Dimensional Materials for Sensing: Graphene and Beyond. *Electron.* **4**(3), 2015, pp. 651.

30. Kuru, C., et al., MoS_2 Nanosheet–Pd Nanoparticle Composite for Highly Sensitive Room Temperature Detection of Hydrogen. *Adv. Sci.* **2**(4), 2015, pp. 1500004.

31. Luo, Y. and Zhang, C., Pt-activated TiO_2-MoS_2 nanocomposites for H_2 detection at low temperature. *J. Alloy. Compd.* **747**, 2018, pp. 550-557.

32. Sarkar, D., et al., Functionalization of Transition Metal Dichalcogenides with Metallic Nanoparticles: Implications for Doping and Gas-Sensing. *Nano Lett.* **15**(5), 2015, pp. 2852-2862.

33. Hao, L., et al., Highly Enhanced H_2 Sensing Performance of Few-Layer $MoS_2/SiO_2/Si$ Heterojunctions by Surface Decoration of Pd Nanoparticles. *Nanoscale Res. Lett.* **12**(1), 2017, pp. 567.

34. Zhang, T., et al., Recent progress in carbon nanotube-based gas sensors. *Nanotechnology*. **19**(33), 2008, pp. 332001.

35. Penner, R.M., A Nose for Hydrogen Gas: Fast, Sensitive H_2 Sensors Using Electrodeposited Nanomaterials. *Acc. Chem. Res.* **50**(8), 2017, pp. 1902-1910.

36. Kong, J., Chapline, M.G., and Dai, H., Functionalized Carbon Nanotubes for Molecular Hydrogen Sensors. *Adv. Mater.* **13**(18), 2001, pp. 1384-1386.

37. Esfandiar, A., et al., $Pd–WO_3$/reduced graphene oxide hierarchical nanostructures as efficient hydrogen gas sensors. *Int. J. Hydrog. Energy*. **39**(15), 2014, pp. 8169-8179.

38. Wang, J., et al., Highly responsive hydrogen gas sensing by partially reduced graphite oxide thin films at room temperature. *Carbon*. **50**(11), 2012, pp. 4061-4067.

39. Russo, P.A., et al., Room-Temperature Hydrogen Sensing with Heteronanostructures Based on Reduced Graphene Oxide and Tin Oxide. *Angew. Chem. Int. Ed.* **51**(44), 2012, pp. 11053-11057.

40. Anand, K., et al., Hydrogen sensor based on graphene/ZnO nanocomposite. *Sens. Actuators B Chem.* **195**, 2014, pp. 409-415.

41. Zhang, Z., et al., Hydrogen gas sensor based on metal oxide nanoparticles decorated graphene transistor. *Nanoscale*. **7**(22), 2015, pp. 10078-10084.
42. Kaniyoor, A., et al., Nanostructured Pt decorated graphene and multi walled carbon nanotube based room temperature hydrogen gas sensor. *Nanoscale*. **1**(3), 2009, pp. 382-386.
43. Chung, M.G., et al., Flexible hydrogen sensors using graphene with palladium nanoparticle decoration. *Sens. Actuator B-Chem.* **169**, 2012, pp. 387-392.
44. Al-Mashat, L., et al., Graphene/Polyaniline Nanocomposite for Hydrogen Sensing. *J. Phys. Chem. C*. **114**(39), 2010, pp. 16168-16173.
45. Shafiei, M., et al., Platinum/Graphene Nanosheet/SiC Contacts and Their Application for Hydrogen Gas Sensing. *J. Phys. Chem. C*. **114**(32), 2010, pp. 13796-13801.
46. Johnson, J.L., et al., Hydrogen Sensing Using Pd-Functionalized Multi-Layer Graphene Nanoribbon Networks. *Adv. Mater.* **22**(43), 2010, pp. 4877-4880.
47. Taghinejad, H., et al., Fabrication and modeling of high sensitivity humidity sensors based on doped silicon nanowires. *Sens. Actuators B Chem.* **176**, 2013, pp. 413-419.
48. Cha, K.H., Park, H.C., and Kim, K.H., Effect of palladium doping and film thickness on the H_2-gas sensing characteristics of SnO_2. *Sens. Actuators B Chem.* **21**(2), 1994, pp. 91-96.
49. Yamazaki, T., et al., Effect of density and thickness on H_2-gas sensing property of sputtered SnO_2 films. *Vacuum*. **77**(3), 2005, pp. 237-243.
50. Windischmann, H. and Mark, P., A Model for the Operation of a Thin-Film SnO_x Conductance-Modulation Carbon Monoxide Sensor. *J. Electrochem. Soc.* **126**(4), 1979, pp. 627-633.